Volume 16, Issue 4, 162421 (1-14)

Iranian Journal of Earth Science (IJES)

https://dx.doi.org/10.57647/j.ijes.2024.1604.21

RUSLE-based model for soil loss modeling and water erosion susceptibility mapping in the Issen basin (west-central of Morocco)

Mohamed Ait Haddou[1,2,*], Belkacem Kabbachi[2], Ali Aydda[2], Youssef Bouchriti[2,3], Jamal Mabrouki[4]

[1]*Department of Geography, Faculty of Humanities and Social Sciences, Ibn Tofail University, Kenitra, Morocco.*
[2]*Department of Earth Sciences, Faculty of Sciences, Ibn Zohr University, Agadir, Morocco.*
[3]*High Institute of Nursing Professions and Technical Health, Agadir, Morocco.*
[4]*Department of Chemistry, Faculty of Science, Mohammed V University, Agdal, Rabat, Morocco.*

[*]**Corresponding author:** mamohamed.aithaddou@uit.ac.ma

Original Research Paper

Received:
21 December 2023
Revised:
16 January 2024
Accepted:
1 February 2024
Published online:
10 February 2024

Abstract:

The Issen basin is the largest sub-catchment area in the southern edge of the Western High-Atlas (WHA) Mountain of Morocco. This basin is characterized by flood flows, orographic and climatic contrast and friable substrate sparsely wooded and covered by heterogeneous vegetation making it vulnerable to soil water erosion. This study aims to evaluate soil loss and to determine the areas susceptible to water erosion in this basin based on the Revised Universal Soil Loss Equation (RUSLE). The RUSLE model was achieved by integrating ancillary and remote sensing data in a Geographic Information System (GIS). The analysis of the obtained map indicates that the erosion rate in the studied basin ranges from 0 to 401 t/ha/yr, with an average of 53 tons/ha/year and a total sheet erosion of 6,886825.87 (tons/year). These results are concordant with the results obtained from other parts of High-Atlas Mountain. Spatially, the erosion differs from a zone to another, where 61.2% of the total study area is lowly to moderately susceptible to erosion (subcritical zones), while the rest (38.8%) is highly to very highly susceptible to erosion (critical zones). The current study indicates that the soil loss in the study area has reached an alarming level and demands fast intervention. Consequently, the identification of critical zones in this work can be useful to prioritize these zones in future environmental planning for treatment against soil loss.

Keywords: Water erosion; Soil loss; RUSLE model; Remote sensing; Issen Basin; Morocco

1. Introduction

Soil erosion by water is a natural process that involves the degradation, transport, and deposition of sediments (Hao et al., 2019). It is considered as a crucial issue in mountainous zones worldwide (Leh et al., 2013; Haregeweyn et al., 2013). The soils of mountainous zones developed in very sensitive environments are subject to anthropogenic and natural disturbances (Stanchi et al., 2015). Water erosion is very active, very damaging and remains the major factor causing dam siltation in semi-arid Mediterranean environments (Ochoa et al., 2016). This phenomenon is particularly severe in Morocco, where 40% of its land is threatened (El Jazouli et al., 2019; Javanbakht et al., 2020). The Moroccan western High-Atlas Mountain is characterized by ecosystem diversity, rich in endemic flora species, and favored mainly by the climatic and orographic contrast that cause a bioclimates variety (Ait Haddou et al., 2022a). Water soil erosion by several rivers, descending from High-Atlas (HA) Mountain; induces ecosystem degradation and dam siltation. The Abdelmomen dam provides drinking water supply in Greater Agadir (9.5 Mm^3) and the irrigation in the Issen basin (13,000 ha). This latter is the largest sub-catchment in the southern edge of the western

High-Atlas Mountain of Morocco. This dam has suffered from silting phenomenon because of rapid land degradation, which estimated by 1,400 tons/km^2/year. The extent of silting phenomenon, especially in semi-arid areas, depends on the physical characteristics of the basin, like topography, lithology, climate, and fluvial system characterized by irregular flooding (Joghatayi et al., 2015; Alahiane et al., 2016). Since 1996, the Moroccan government elaborated a national program to combat ecosystem degradation caused by water erosion, called the National Watershed Management Plan (PNABV) (HCEFLCD, 2011).

The soil erosion and its impacts are currently one of the main concerns for policy makers and watershed managers. Soil erosion modeling plays an important role in designing and implementing soil conservation and management strategies (Panagos et al., 2015; Jehangir Khan et al., 2021). As such, effective modeling can provide information on soil loss and its trends (Ganasri and Ramesh, 2016). Models vary considerably in their parameters, application and results (Merritt et al., 2003).

In general, several empirical GIS-based models were proposed to assess annual soil loss and to map vulnerable areas to water erosion in mountainous zones, such as Universal Soil Loss Equation (USLE), Modified Universal Soil Loss Equation (MUSLE), Revised Universal Soil Loss Equation (RUSLE) (Wischmeier and Smith, 1978; Renard, 1997; Bensekhria and Bouhata, 2022), and Erosion Potential Model (EPM), (Gavrilović, 1972; Amini et al., 2010; Ebadati et al., 2022). These models needs small amount of input data and simple formulation, but are still applied in various basins with similar climatic and geo-environmental conditions. The evaluation of the efficiency of these models was reviewed; the RUSLE and other models showed highly better results in sediment yield estimation than EPM model, especially, for arid and semi-arid environments (Amini et al., 2014).

RUSLE, derived from USLE, is one the most widely used water erosion models, which is recently being applied on catchments in a wide set of arid and semi-arid environments (Rezapour Tabari and Yazdi, 2014; Getu et al., 2022; Kifelew et al., 2022; Saha et al., 2022). The RUSLE model has been widely applied on many African catchments (Mhangara et al., 2012; Ligonja and Shrestha, 2015; Getachew et al., 2021). The RUSLE model has proved as a useful tool for national and regional policy-making to conserve and restore soil (Ustaoğlu et al., 2021).

In Morocco, the USLE/RUSLE model remains the most widely used model (51.32%). However, the EPM is rarely used in the literature (2.63% only) (Lamane et al., 2022). In addition, the RUSLE model requires least number of input data. Commonly, this model demands five essential input factors for soil loss estimation, including rainfall (R), topography (soil Loss and Steepness (LS)), soil erodibility (K), cover management (C), and support practice (P). Except for the K factor which needs laboratory analysis, the other factors can be easily derived from remotely sensed data that is recently available free of charge (Aswathi et al., 2022). The tremendous benefit from the remotely sensed data is largely reflected by continuous increase of studies using it.

In Morocco, several authors attempted successfully to estimate the annual soil loss and to identify the degraded soil in various catchments over the High-Atlas Mountain using RUSLE model (Ayt Ougougdal et al., 2020; Meliho et al., 2020). So far, no study has been evaluated water erosion in the Issen basin by using one of the aforementioned GIS-based models, including the RUSLE model. In our knowledge the direct siltation measurement in Abdelmoumen dam, which is located in downstream of the studied basin, is the only estimation of soil loss in this basin. In addition, according to PNABV, the quantification of water erosion in this basin is necessary due to facies vulnerability, pedoclimatic hazards, atmospheric disturbances frequency, and steppisation of argan tree pre-forests in this area. Consequently, modeling soil erosion at the Issen catchment scale using GIS-based model will be useful to precise soil loss estimation, to map the most several threatened areas, to combat gully erosion in the whole basin, and then to probably reconcile the environmental impacts of erosion on the water storage capacity in the Abdelmomen dam.

Thus, in this study, the RUSLE soil erosion model was used to quantify the annual soil loss and to map the areas susceptible to water erosion in the Issen basin. More precisely, the study put forward priority areas that need fast intervention. Also, this study offers a general comparison of the annual soil loss rate in Morocco.

2. Study area

The Issen basin, as part of the downstream section of the Souss Wadi, is the largest sub-catchment area of the southern edge of the Western High-Atlas (WHA) that marks the Southern Atlas furrow. This basin covers an area of 1,300 km^2 and extends over 60 km in length and 35 km in width following the NE-SW orientation (Ait Haddou et al., 2022b; Ait Haddou et al., 2022c) (Fig. 1).

In general, the climate of this basin is of a medium arid to upper semi-arid Mediterranean type, varying from "warm" over most of the Argana corridor and the south Atlas Mountains to "cool" over the High-Atlas Mountains edge. The rainfall in this basin is irregular, varying between 200 and 500 mm/year with an interannual average of about 302 mm/year. The coefficient of variation (Cv) equals 67%, reflecting a high variability of rainfall during the last 37 years (1981-2017) (Ait Haddou et al., 2020). The average annual temperature is about 21.85 °C. The evaporation losses from the Abdelmomen dam storage area are about 2,278 mm/year.

From geological point of view, the studied basin can be divided into three different zones (Tixeront and Duffaud, 1977) (Fig. 2): (i) Ancient primary massif (Zone 1) consists of the schists and the quartzites and corresponds to Blad Demsira, Ida O'Mahmoud, and Ida O'Zal; (ii) Argana Permo-Triassic corridor (Zone 2) comprises at least 2,500 m of fluvial, lacustrine, and coarse to fine clastic floodplain deposits (Olsen et al., 2003) that consist of red sandstone-silty and conglomeratic detrital Formation. The Argana Permo-Triassic corridor forms broad troughs crisscrossed by sandstone monoclinal ridges and controlled by an extensive fault system (Mlih et al., 2004); and (iii) Jurassic

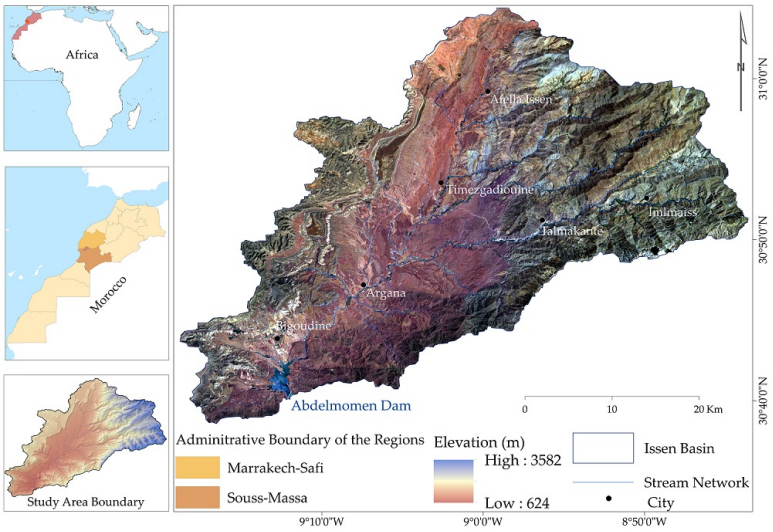

Figure 1. Location of the study area.

limestone and marl-limestone plateaus (Zone 3) correspond to the northern cuestas of Ida O'Bouzia, which is classified as one of the meridional highlands of Ida O'Tanan and Ida O'Souar.

Moreover, according to the only existing pedological sketch of Morocco (Cavallar, 1950), there are two soil classes in the Issen basin. The Calcisols (red mountain forest soils), covering 61% (about 79,422 ha) of the total basin, consist of slightly leached or calcareous eroded soils associated with humiferous-carbonated soils. The Leptosols (brown and red soils), covering 34% (about 44,268 ha) of the total basin, consist of brown forest soils, eroded soils, and desertic bare rocky on the Paleozoic rocks, and are sparsely wooded and covered by heterogeneous vegetation.

3. Materials and methods

3.1 RUSLE model

In the present study, mapping soil susceptibility to water erosion and computing soil loss (A) rate were investigated using the RUSLE model. The used model involves a combination of five important water erosion factors related to rainfall erosivity, soil erodibility, topography, land cover, and anthropogenic protection practices (Fig. 3), as shown in Equation (1) (Renard, 1997). In general, these factors vary in space and time and are depend on other input factors

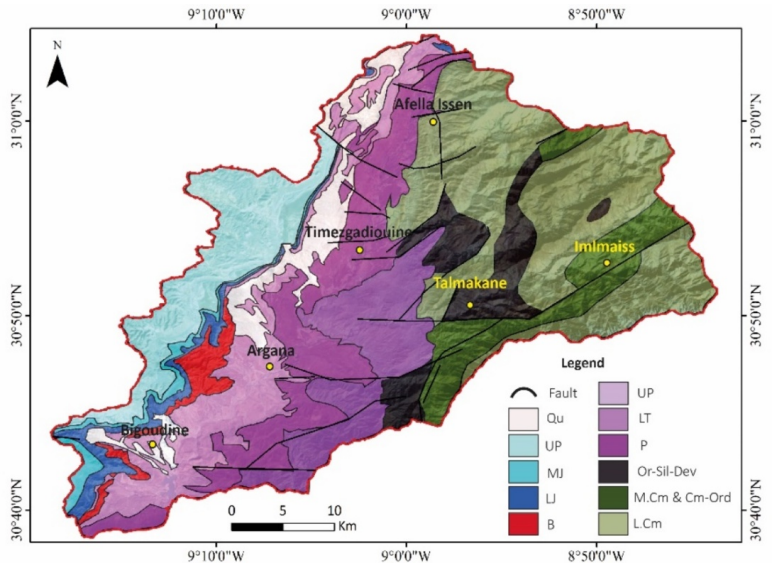

Figure 2. Lithological units of the Issen basin (1:100.000). Of note that this map was digitalized from an assembly of two geological maps of Argana and ImiN'Tanoute (Tixeront and Duffaud, 1977). (In this map, the Palaeozoic massif completed as an approximation by the geological map of ImiN'Tanoute). Abbreviations; Qu: Quaternary, UJ: Upper Jurassic, MJ: Middle Jurassic, LJ: Lower Jurassic, B: Basalt, UT: Upper Triassic, LT: Lower Triassic, P: Permian, Or-Si-Dev: Ordovician Silurian-Devonian, M. Cm & Cm-Ord: Middle Cambrian & Cambro-Ordovician, L.Cm: Lower Cambrian) (Ait Haddou et al., 2023).

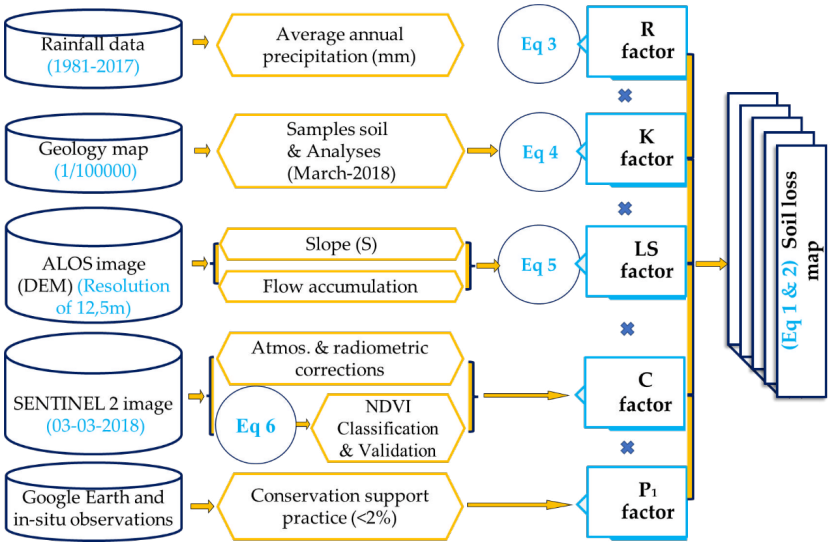

Figure 3. The methodological flowchart of the used model.

(Phinzi and Ngetar, 2019).

$$A = R \times K \times LS \times C \times P_1 \quad (1)$$

where R is rain erosivity factor (MJ.mm/ha.h.yr), K is soil erodibility factor (t.h/MJ.mm), LS is topographic factor (L is slope length (m) and S is slope steepness (%)), C is a land cover factor, and P_1 is erosion control practice factor. Note that; MJ (megajoule), mm (millimeter), ha (hectares), h (hour), yr (year), m (metre), and t (ton).

In the present study, the model was implemented in a free GIS platform (QGIS 2.18). Firstly, the aforementioned factors were prepared as separate raster maps using QGIS software. Then, all obtained maps were adjusted at 12.5 m resolution. Finally, the global precision of the model was calculated using Equation (2) (Abaoui et al., 2005) based on in-situ observations covering all soil loss classes (7 control points for each soil class were acquired to achieve the precision).

$$Pg = \frac{PCv}{PCt} \quad (2)$$

where Pg is global precision, PCt is the total number of control points, and PCv is the number of valid control points in the field.

3.2 *R* factor or rainfall erosivity

The R-factor is strongly linked to soil loss that varies spatially and temporarily (Talchabhadel et al., 2020). It is the most important factor for estimating erosion response to climate (Khemiri and Jebari, 2021). The rainfall erosivity factor was calculated using Equation (3) (Renard and Freimund, 1994), which is frequently used to highlight the correlation between the R-factor and precipitation (Mukanov et al., 2019).In this study, the annual and monthly average rainfall data recorded in 13 stations for the period 1981-2017 was collected from local agencies and authorities [Souss Massa Hydraulic Basin Agency (SMHBA), Tensift Hydraulic Basin Agency (THBA), and High Commission for Water and Forests and the Fight against Desertification, Morocco (HCWFFD)] and used to calculate R factor. To obtain the R factor raster map, the obtained R values were spatially interpolated using spline interpolation method implemented in geostatistical analysis tools in QGIS.

$$R = 0.04830 \times P^{1.610} \quad \text{for}(P < 850 \ \text{mm/year}) \quad (3)$$

where R is the rainfall aggressivity index (MJ.mm/ha.h.yr), and P is the annual average rainfall (mm/year).

3.3 *K* factor or soil erodibility

The K-factor (t.h/MJ.mm) expresses the intrinsic susceptibility of soil particles to be detached and consequently transported by surface runoff (Fernandez et al., 2003). The soil erodibility factor was calculated according to the Wischmeier and Smith equation based on the physical properties of soil, including the percentage of organic matter and the percentage of sand, silt, and clay (Eq. (4)).

$$K = 27.66 \times m \times 1.14 \times 10 - 8 \times (12 - a) + 0.0043 \times (b - 2) + 0.0033 \times (c - 3) \quad (4)$$

where K is soil erodibility (t.h/MJ.mm), m is soil texture (% fine sand + %Silt) × (100 − % clay), a is the percentage of the organic matter, b is soil structure code, in which class (1) is very structured or particulate, class (2) is fairly structured and class (3) is slightly structured, and c is permeability in which class (1) is rapid, class (2) is moderate to rapid and class (3) is moderate.

Practically, to obtain K factor values, the texture, organic matter, structure, and permeability of about 26 soil samples collected from the field, in March 2018, were analyzed in the laboratory. To obtain the soil erodibility raster map, the K-adjusted values were spatially interpolated using Inverse Distance Weighted (IDW) geostatistical analysis method in QGIS.

3.4 *LS* factor

The slope length or slope steepness shows the topographical influences on soil erosion (Ghosal and Das Bhattacharya, 2020), substantially affects sheet and rill erosion (Bosco

et al., 2015). *LS* factor was computed by combining slop and flow accumulation maps as expressed in Equation (5) (Mitasova et al., 1996). These maps were created from the Digital Elevation Model (DEM) of 12.5 m resolution using QGIS software. The DEM was captured by Advanced Land Observing Satellite (ALOS) and collected from the site web of the Japan Aerospace Exploration Agency (JAXA). The LS factor was then computed using the "Raster Calculator" tool according to the Mitasova methodology.

$$LS = (\text{Pow}\frac{\text{Flow accumulation} \times \text{resolution}}{22.1, 0.6}) \times (\text{Pow}\frac{\sin(\text{slope}) \times 0.01745}{0.09, 1.3}) \quad (5)$$

where *LS* is the length–slope steepness factor, the resolution is the size of the grid cell, and sin slope is the slope degree value in sin.

3.5 *C* factor or Land cover

C Factor contributes to find the combined effect of all interdependent land use/land cover variables (Wischmeier and Smith, 1978). The *C* factor is essentially related to nature and the density of vegetation cover. In the literature, the vegetation cover can be estimated using satellite image data. Normalized Difference Vegetation Index (NDVI) is one of the most used vegetation indices to map vegetation cover and vegetation health (Benavidez et al., 2018). Knijff et al. (2000) studied the relationship between the *C* factor and NDVI. They reported that the NDVI values vary between −1 and 1, where low values indicate areas with low vegetation cover (e.g., bare soil, built-up, water bodies, cultivated areas) that correspond to high values of *C* factor, and high values indicate areas with dense vegetation (e.g., forest,) that correspond to low values of *C* factor.

NDVI can be computed by combining the near-infrared band and the red band as shown in the following Equation (6).

$$\text{NDVI} = \frac{(\text{PNIR} - PR)}{(\text{PNIR} + PR)} \quad (6)$$

In this study, we collected a multispectral Sentinel 2*A* scene captured on March 03rd 2018 from the European Space Agency (ESA). NDVI was extracted after applying an atmospheric correction on the collected data by using Dark Object Subtraction (DOS) algorithm. Then, a land cover map was generated by applying maximum likelihood supervised classification on the obtained NDVI map based on five regions of interest (ROIs) (water, dense forest, clear forest and matorrals, cultivated land, and bare land). The classification was verified by using high-resolution Google Earth images. Finally, to generate the RUSLE model each land cover class was attributed to a numeric value as shown in Table 1. Of note, these steps were achieved by using QGIS software.

3.6 *P* factor or Erosion control practice

P factor refers to the effect of water and soil conservation practices on the erosion rate, which depends on cultivation practices and that of up-and-down slope cultivation (Kang et al., 2001). The *P* values are between 0 and 1. The value close to 0 indicates good conservation practice and the value close to 1 indicates poor conservation practice (Ganasri and Ramesh, 2016). In this study, due to rare conservation practices of the cultivated areas, (less than 2% in the whole basin area), and the absence of studies reporting land management maps or significant conservation measures (*P* factor) for the study area, we assigned usually the value 1 to the *P* factor reported in the literature (Gaubi et al., 2017; Aouichaty et al., 2022).

Table 1. *C* factor values for each land use type used in this study (Brahim et al., 2020; Labbaci et al., 2020).

Land use	Value of the *C* factor
Water	0.00
Dense forest	0.01
Clear forest and Matorrals	0.16
Cultivated land	0.50
Bare land	1.00

4. Results and discussion

4.1 *R* factor

The results of the *R* factor reveal a spatial variability; where it is about 232.5 MJ.mm/ha.h.yr in the central part of the basin (Bigoudine and Timzgadiouine), and it is more than 1,213.7 MJ.mm/ha.h.yr in the periphery of the basin (the upper Ida O'Mahmoud valley, the Ida O'Zal massif in the south and southeast, and the western plateaus) (Table 2 and Fig. 4). The average rainfall erosivity is about 537.64 MJ.mm/ha.h.yr for the whole basin. Furthermore, about one-half of the basin area suffers from rainfall erosivity, estimated at more than 700 MJ.mm/ha.h.yr. Commonly, the areas of dry warm summers of the Mediterranean climate zones have mean erosivity values lower than 2,000 MJ.mm/ha.h.yr (Panagos et al., 2017).

4.2 *K* factor

K factor values range from 0.015 to 0.079 t.h/MJ.mm with an average of about 0.042 (Table 3 and Fig. 5). 18.31% of the soil in the Issen basin is slightly erodible, while 20.64%

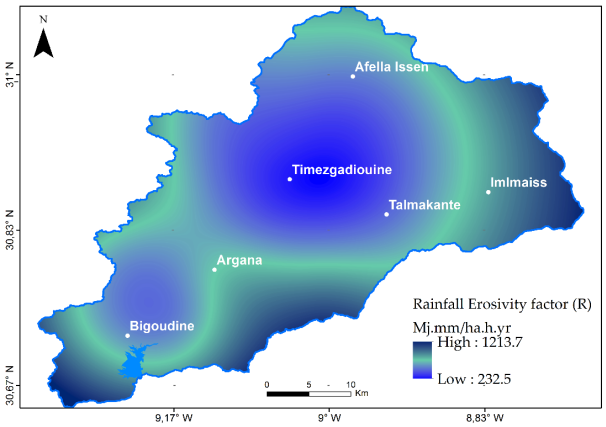

Figure 4. Spatial distribution of the rainfall erosivity (*R* factor).

Table 2. The list of meteorological stations shows spatial locations, the mean annual rainfall (*A.R.*) (mm/year), the average *R* factor value (MJ.mm/ha.h.yr), and the bioclimatic zones.

Meteorological station	Longitude (West)	Latitude (North)	Annual rainfall	*R*-factor	Bioclimatic zone
Abdelmomen dam	9.190°	30.670°	402.06	753.10	Middle semi-arid
Agunza	9.153°	30.751°	253.74	358.93	high arid
Argana	9.122°	30.778°	349.70	601.50	Lower semi-arid
Amsoul	9.069°	30.842°	193.80	232.52	lower arid
Tizguine	9.120°	30.918°	236.63	320.80	Middle semi-arid
Iloudjane	8.801°	31.183°	332.20	553.72	Lower semi-arid
Aghbar WHA	8.367°	30.880°	537.40	1201.50	High semi-arid
TiziOuMaacho	8.968°	31.058°	465.50	953.40	Middle semi-arid
Ikakern	8.975°	30.832°	222.73	291.00	Middle-arid
Timlilt	9.139°	31.033°	344.00	585.90	Lower semi-arid
Dkhila dam	9.285°	30.569°	307.70	489.51	Lower semi-arid
Ain Asmama	9.286°	30.773°	473.72	980.70	Middle semi-arid
Immouzzer	9.400°	30.670°	540.80	1213.70	High semi-arid

NB: Geographic Coordinate System (GCS-WGS-1984, Units: Decimal Degrees).

is moderately erodible. The moderately erodible soil covers the western piedmonts of the ancient massif (eastern part of the basin) and the limestone plateaus (western part). However, more than 61.1% of the soil is highly erodible of which 23.60% is very highly erodible, covering the Argana basin, Timzgadiouine basin, and the high basin (Triassic depression).

4.3 *LS* factor

The slope distribution results reveal five classes covering areas ranging from 7864 to 35403 ha (Fig. 6). The moderate and steep slopes (3 to 30%) are predominant while the low slopes ($< 3\%$) cover less area of the basin. Generally, the whole basin is relatively sloping land, except for the Argana corridor and the extreme northwest of the basin (Blad Demsira).

Fig. 7 shows the *LS* factor results. The low values of *LS* ($0.05 - 5$) indicate the areas of low susceptibility to erosion, which is observed in the Argana corridor, in the northern cuestas, and along the channel of the Issen Wadi. Whereas the highest values (> 20) indicate the areas of high susceptibility to erosion, corresponding to the ancient massif at the east, the glacis of the Jurassic coast, the southwestern mountain ranges, and the meridional plateaus at the west, which cover more than 32.00% of the total area of the basin. The *LS* factor average value is about 6.83 for the whole basin.

4.4 *C* factor

The analysis of the *C* factor map reveals that one-third (33.33%) of the total basin area had values > 0.7, which are observed in the central and upstream parts (Fig. 8) and corresponding to soils without perennial vegetation due to the unfavorable climatic and edaphic conditions. The average value of the *C* factor is 0.35, corresponding to bare soils covered by the matorral and tree steppes (e.g., Argan groves). The low value of the *C* factor is about 0.01, corresponding to the areas surrounding the Argana corridor at the meridional plateaus and the west and the northwest sides of the High Atlas.

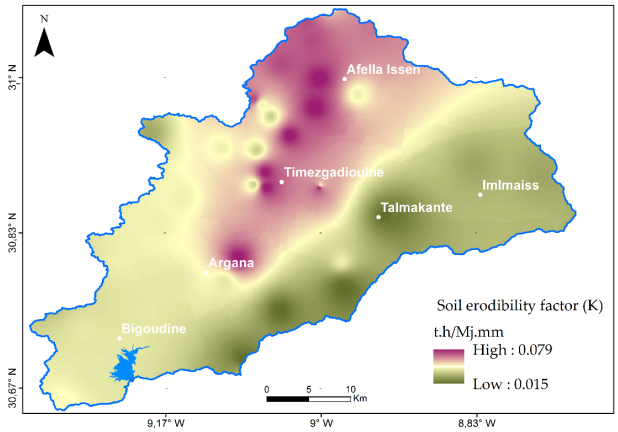

Figure 5. Spatial distribution of the soil erodibility (*K* factor).

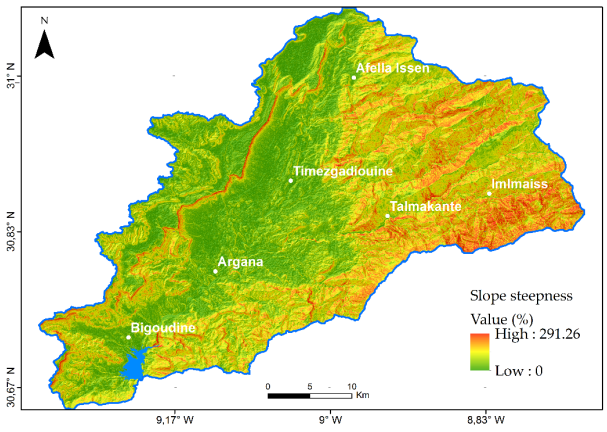

Figure 6. Spatial distribution of the slope gradient (*S*) in the study area.

Table 3. Characteristics and physical properties of soil samples and calculation of erodibility (*K*).

Sites	Long. (West)	Lat. (North)	Coarse sand %	Fine sand %	Coarse silt %	Fine silt %	Clay %	Organic matter %	Structure code	Perm-eability class	K (t.h/MJ.mm)
E1	9.044°	30.75°	59	11.22	3.92	11.96	10.94	3.01	2	2	0.015
E2	9.042°	31.015°	8.93	37.5	20.96	18.86	12.7	1.06	2	2	0.067
E3	9.213°	30.804°	30.93	4.4	12	31.45	20.6	0.65	3	3	0.042
E4	9.034°	30.938°	9.8	20.86	28.3	28.18	12.5	0.39	3	3	0.079
E5	9.347°	30.571°	26.05	21.26	17.9	17.46	15.46	1.94	3	3	0.048
E6	9.054°	30.958°	29.82	8.82	5.13	34.98	20.6	0.65	2	2	0.035
E7	9.06°	30.898°	9.8	20.76	28.3	28.3	12.5	0.39	3	3	0.079
E8	9.002°	30.999°	11.23	19.12	27.45	29.3	12.4	0.49	3	3	0.077
E9	9.153°	30.785°	19.32	27.65	12.9	16.8	21.8	1.59	2	2	0.039
E10	9.059°	30.882°	12.22	19.6	29.8	26.7	11.2	0.47	3	3	0.078
E11	9.104°	30.781°	41.15	24.3	15.59	6.8	11.7	0.44	2	2	0.039
E12	8.763°	30.896°	39.67	9.23	9.02	16.2	24.9	0.97	3	3	0.028
E13	9.187°	30.745°	28.5	9.02	20.39	16.2	24.9	0.97	3	3	0.037
E14	9.207°	30.714°	26.96	24	11.7	15.7	20.33	1.36	2	2	0.035
E15	9.248°	30.683°	41.15	24.3	15.59	6.8	11.7	0.44	2	2	0.039
E16	9.077°	30.932°	20	38.42	6.83	15.5	18.95	0.36	2	2	0.049
E17	9.255°	30.727°	40.02	26.35	7.13	10.18	16.12	0.28	2	2	0.034
E18	8.919°	30.012°	10.27	8.27	11.33	30.83	34.53	4.81	3	3	0.025
E19	8.829°	30.850°	62.04	15.06	3.86	8.8	9.54	0.72	2	3	0.023
E20	8.961°	30.982°	38.44	21.4	11.93	14.23	13	1	3	3	0.045
E21	9.064°	30.971°	40.49	15.23	16.24	13.99	13.58	0.5	2	2	0.037
E22	9.176°	30.845°	22	13.03	18.5	23.16	20.31	3.07	3	3	0.039
E23	9.088°	30.682°	31.19	8.3	7.27	30.8	20.7	1.74	3	3	0.037
E24	8.978°	30.802°	27.58	31.92	15.16	9.53	13.2	2.66	3	3	0.046
E25	8.946°	31.057°	21.2	34.71	4.9	26.81	10.87	1.53	2	2	0.055
E26	8.999°	31.084°	40.48	15.2	16.14	13.99	13.54	0.54	2	2	0.036

4.5 Erosion susceptibility map

The final annual soil loss estimation, as described above was determined by multiplying the respective RUSLE factors, *R* factor, *K* factor, *LS* factor, and *C* factor, using a raster calculator in QGIS. The annual soil loss in the study area was reclassified into four categories according to the FAO soil classification system or standards. These classes are low (0 – 10 t/ha/yr), moderate (10 – 25 t/ha/yr), high (25 – 45 t/ha/yr), and very high (> 45 t/ha/yr) soil erosion classes. Figs. 9 and 10 show the obtained map and the percentage of the erosion classes. The water erosion rate ranges from 0 to 401 t/ha/yr and its average is about 53 t/ha/yr. The analysis of the erosion map indicates that 61.14% of the total basin area is lowly to moderately susceptible to erosion (subcritical zones), while the rest (38.87%) is highly to very highly susceptible to erosion (critical zones). The critical zones correspond to areas that lose more than 25 t/ha/yr that are located in the upstream part of the basin. Furthermore, 52.9% of the subcritical zones correspond to slightly eroded areas, while the rest (8.25% about 10,725 ha) correspond to moderately eroded areas that lose 10 to 25 t/ha/yr that are located in the downstream part of the basin.

The resulting soil loss prediction map was validated to assess the accuracy of the model. The validation process

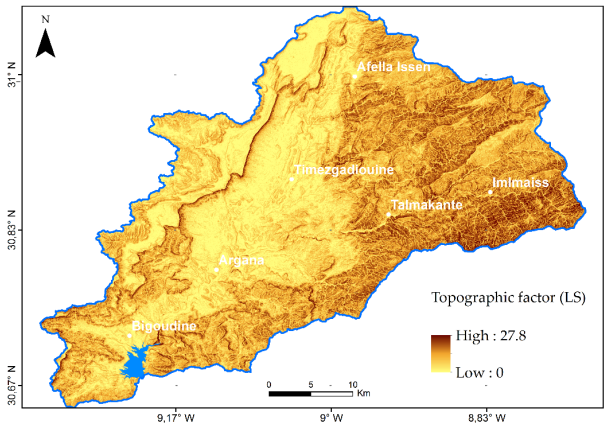

Figure 7. Spatial distribution of the topographic factor (*LS*).

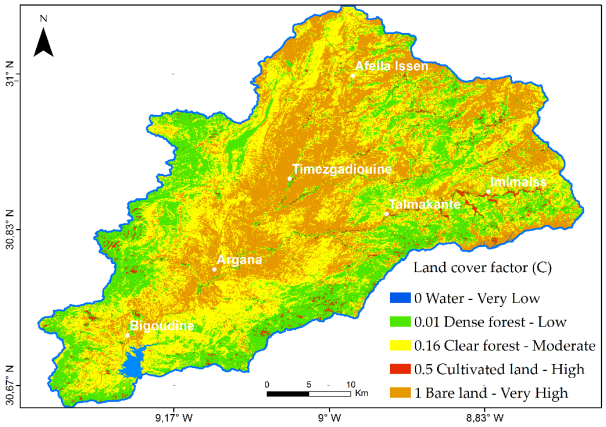

Figure 8. Spatial distribution of the land cover factor(*C*).

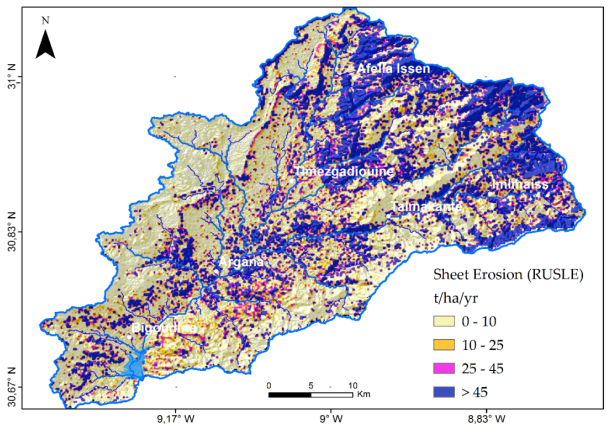

Figure 9. Water erosion rate (A) in the Issen basin using the RUSLE model.

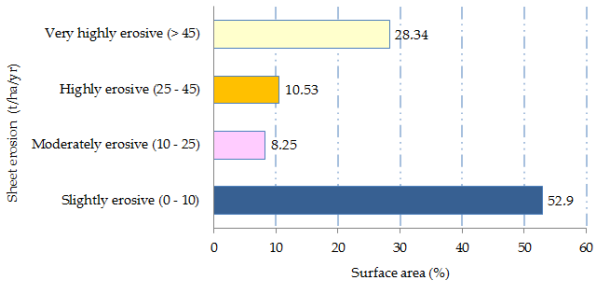

Figure 10. Annual soil erosion rate distribution in the Issen watershed according to the RUSLE model.

involves a three-way comparison between the final erosion map and field direct observations. The global precision of the used model is about 71.41% (Table 4).

The results of the used model revealed that the whole basin was affected by water erosion phenomena with a total soil loss of about 7 gigatons/year, which is more than that estimated indirectly through silting of the Abdelmomen dam (14 t/ha/yr). Commonly, water erosion becomes active on slopes above 3% (Fistikoglu and Harmancioglu, 2002). Consequently, 94% of the Issen basin is susceptible to erosion. The soil susceptibility to erosion differs from one region to another in this basin depending on the influence of the RUSLE model factors. The highly and very highly susceptible soils correspond to schistose and detrital facies, which are observed in the upstream part of the basin and in the center of the Argana corridor. The erodibility of these facies was estimated at 0.015 to 0.079 t.h/MJ.mm. Furthermore, the C factor ranges from 0.16 to 1, revealing a clear fragility and a high susceptibility to ablation. In addition, the C factor is more than 0.5 in the center of the Argana corridor due to anthropogenic activities (overgrazing and rapid deforestation of argan forests), which may be caused by desertification phenomena. Commonly, the semi-arid Mediterranean climatic conditions cause landslides, especially, in the zones of low to medium forest cover density in an accentuated topographic terrain that has an LS factor value > 10. That is the case of the central High Atlas massif (Ait Driss, Ouargioun, Ait Chaib, and Ait Bkhayr) where the altitude is about 3,528 m, and the Jurassic plateaus of the Western High-Atlas where the altitude ranges between 1,100 and 1,270 m.

The western and southeastern parts of the basin are slightly susceptible to water erosion due to the low slope, the soil's nature, and the forest cover. The western part is characterized by the presence of moderately evolved soils with mixed matorral cover (argan, thuja, juniper, and evergreen oak), which have an erodibility index of about 0.035. The soils in the southeastern part are metamorphic hard rock's of the ancient massif (primary schists and sandstones), which have an erodibility index (K) less than 0.025 t.h/MJ.mm, and a cover index (C) of about 0.01. The rest of the basin (8.25%) is moderately susceptible to water erosion because of the degradation of the vegetation cover. Zhao et al. (2019) indicated that the argan tree landscape degradation in southwest Morocco due to climatic conditions and anthropogenic activities may increase erosion.

The regression of LS, R, C, and K factors with water erosion rate (A) revealed a strong correlation between the soil loss rate and the topographical factor (LS) with ($R^2 = 0.78$) (Table 5). A slight correlation is observed between soil loss rate and rainfall erosivity (R) with ($R^2 = 0.54$) followed by the C factor. In general, several studies reported that erosion decreases with increasing vegetation cover. In contrast, other studies highlighted that sediment yield of watersheds and gullies have no correlation with vegetation cover (Rey et al., 2004). This result is consistent with those obtained from other watersheds in Moroccan that have similar geoenvrionmetal conditions.

Table 4. Risk class, their degree of environmental hazard, and the global precision of the model.

Risk of water erosion	Control points	Degree of environmental hazard	Degree of accuracy (%)	Global Precision (%)
Slightly erosive	7	No dangerous	57.14	71.41
Moderately erosive	7	Moderate dangerous	42.28	
Highly erosive	7	Dangerous	100.00	
Very highly erosive	7	Highly dangerous	85.71	

Table 5. The relationship between soil erosion rate (A) and water erosion factors (R. LS. K. C.).

Factors	Soil erosion rate (A)	Erosivity factor (R)	Topographic factor (LS)	Erodibility factor (K)	Vegetation cover factor (C)
A	1	***	***	***	***
R	0.545	1	***	***	***
LS	0.784	0.180	1	***	***
K	0.093	-0.422	0.281	1	***
C	0.451	-0.600	0.123	0.484	1

The obtained results are concordant with other studies. Table 6 compares the results of the RUSLE model application in the WHA, including the results of the present study:

• The erosion rate estimated in the Biological and Ecological Interest Site (BEIS) of Ain Asmama (WHA) ranges from 0.1 to 339.03 t/ha/yr with an average of $50-60$ t/ha/yr (Labbaci et al., 2020). The studied zone bordering our study area is morphologically characterized by the alternate flat and very escarped terrain, and climatically characterized by an aggressiveness index range from 46 to 96. The soils of the studied zone are non-devolved, highly erodible, very low permeable, and have an erodibility index ranging between 0.23 and 0.58 (average of about 0.4).

• The average erosion rate in the Tifnout Askaoun, covering an area of about 1488 km^2, is about 14.44 t/ha/yr (Tairi et al., 2021). They noted the resistance of the crystalline terrain to water erosion ($K = 0.044$) in the upstream part, the other factors ($LS = 17.05$, $R = 94.58$, and $C = 0.23$) conducted strong erosion, and then, high soil loss in the downstream part of the basin. Effectively, these studies confirm that LS, R, and K factors contribute to erosion more than C and P factors.

• The erosion rate in the Beni Mohand basin, which is located in the middle part of the Oued Souss, ranges from 0 to 227.67 t/ha/yr (average of about 40.38 t/ha/yr) and the soil loss rate is about 1.4 million tons/year (Bou-imajjane and Belfoul, 2020). They reported that the most affected areas are located in the upstream part of the basin, which is characterized by moderate to steep slopes, high rainfall, denuded lands, and friable soils.

• The erosion rate in the Tensift basin (WHA) was estimated at 44.03 t/ha/yr. Its ranges between 10.52 and 132.25 t/ha/yr, respectively, in the Haouz plain and the High Atlas with standard deviation of 87.96 t/ha/year (Meliho et al., 2020). Their research concluded that 30.43% of the total Tensift basin is high-to-extremely-high soil losses. Soil erosion is light in the Haouz plain and high-to-extremely high in the High Atlas of the Tensift watershed, which due to the topographic factor (LS). This factor is the most important environmental factor contributing to the high rates of soil erosion and affects the R factor. In Tensift basin, the slope gradient and LS factor are correlated with soil erosion with correlation coefficient of 0.57 and 0.55, respectively.

In addition, Table 7 lists the results of the water erosion rate in the other belts in Morocco. Ayt Ougougdal et al. (2020) studied water erosion in Ourika, which is located on the northwestern side of the High Atlas of Marrakech, Morocco. They reported the great variability of the erosion factors conducting a high erosion rate in the studied area (average of about 258.48 t/ha/yr). About 62.06% of the total area lost more than 35 t/ha/yr of soil because of high humidity, very steep slope, and very friable lithology (marl with rare plant cover) of the terrain. Elaloui et al. (2017) estimated that the erosion rate in the Tessaoute basin (part of the CHA) ranges from 0 to 9,350 t/ha/yr. They reported that the average annual soil loss is about 15.44 t/ha/yr and the slope,

Table 6. The comparison of average RUSLE factors and soil loss in the WHA.

Watershed	R	K	LS	C	P	Erosion rate (t/ha/yr)	Source
Issen	527.64	0.042	6.83	0.35	1	53	This study
TifnoutAskaoun	94.58	0.044	17.05	0.23	0.85	14.44	(Tairi et al., 2021)
Beni Mohand	35-44	0.017-0.022	0-664	0.05–0.7	0.8	40.38	(Bou-imajjane and Belfoul, 2020)
Ain Asmama	46-96	0.23-0.58	> 30	0.01-1	0.5	0.1-339	(Labbaci et al., 2020)
N'fis	62-112	0.05-34	0.01-68	0.6	> 0.5	44.03	(Meliho et al., 2020)

Table 7. Comparative table of the average soil loss by using the RUSLE model in Morocco.

Region	Watershed	Area (Km^2)	Erosion rate (t/ha/yr)	Source
Central High-Atlas	Ourika	503	258.48	(Ayt Ougougdal et al., 2020)
Central High-Atlas	Tessaoute	1418.35	15.44	(Elaloui et al., 2017)
Northwestern Rif	Kharroub	426.70	52.17	(Tahiri et al., 2017)
Eastern Pre-Rif	Oued Tlata	123.15	61	(Tribak et al., 2009)
Eastern Rif	Boussouab	252.20	55.35	(Sadiki et al., 2004)
Northern Morocco	Rif basin	16010	27.7	(Salhi et al., 2020)

erodibility, and vegetation cover factors are more affecting the erosion phenomena. Tahiri et al. (2017) reported that the annual soil losses in the Mharhar and Kharroub basins of the northwestern Rif are about 64.86 t/ha/yr and 52.17 t/ha/yr, respectively. Consequently, the high susceptibility to water erosion in the High-Atlas belts may be due to the soil friability (silt, loess, and so on), very steep slope, and rainfall intensity in this area.

The present study and the aforementioned studies showed the importance of the used model for estimating the water erosion rate in Morocco. Furthermore, the majority of these studies reported that the highly susceptible areas to erosion risk correspond to areas where the values of the RUSLE factors are high (rainfall, topography, land cover, and so on). It is important to report that the average annual soil losses are unevenly distributed over Morocco, which may be due to the input data uncertainties during pre-processing, interpolation, and resolution conversion (Lu et al., 2004). Nevertheless, the obtained results can be useful tools for environmental planning against erosion risk and predicting flooded areas to minimize their risk. In addition, the used model can be useful to map erosion risk in other areas not yet investigated in Morocco such as the southern Atlantic side of the Souss Oued.

In contrast, the impact of monthly rainfall on soil loss and its impact on land use/land cover in the Issen catchment should be assessed continually. In fact, expressing the impact of land use change on soil erosion it is necessary to develop new methods for assessing the potential of sediment generation in the sub-basins of the Issen watershed. Further, in order to ensure sustainable land use and comprehensive watershed management, it is necessary to develop new methods for assessing the impact of land use change on soil erosion. These limitations suggest the need for further studies to test other techniques such as radioactive markers Cesium-137 (137Cs) and Machine Learning (ML) models that become outstanding approach for soil loss rate estimation.

5. Conclusion

A GIS-based RUSLE model was used to evaluate the soil loss rate and to determine the areas susceptible to water erosion in the Issen basin (WHA of Morocco). Effectively, the analysis of the obtained map indicates that the erosion rate in the study area ranges from 0 to 401 t/ha/yr (an average of 53 t/ha/yr), with a total sheet erosion of 6,886825.87 (tons/year), indicating that the study area has reached an alarming level of soil loss. 61.2% of the total basin area is lowly to moderately susceptible to erosion (subcritical zones), while the rest (38.8%) is highly to very highly susceptible to erosion (critical zones). The high value of the soil loss achieved in this study may be explained by the physical characteristics of the basin. The study area is characterized by the presence of friable soils of the Permo-Triassic Formation (clayey-detritic), more than 46% of the study area has a steep slope, more than 50% of the study area is characterized by moderate rainfall aggressiveness, and degraded plant cover because of anthropogenic activities (deforestation and absence of clear biological reserve conservation strategy). In addition, the used model helps us to identify the priority areas that need preservation against water erosion risk. The obtained results can be a useful tool for environmental planning against erosion risk and predicting flooded areas to minimize their risk. Our study is the first attempt to use the RUSLE model integrated with GIS and RS to investigate the annual soil erosion rates in the Issen catchment. We have shown that, especially in regions with insufficient data, the GIS-based RUSLE model can be an effective tool for quantifying soil loss due to soil erosion. This model offers a clear and important map shown the spatial distribution and quantitative estimation of soil loss that could plays an essential guidance for planning soil and water conservation measures. This model can also be applied to other similar basins of the central-western region in Morocco and other regions in the arid and semi-arid basin at regional and national scale.

Acknowledgments

The authors would like to thank Japan Aerospace Exploration Agency (JAXA) and European Space Agency (ESA) for making satellite data available free of charge. The authors also would like to appreciate the efforts of the QGIS Development Team in making the software free for use. Furthermore, a big thanks to the local agencies and authorities (ABHSM, ABHT, and HCEFLCD) for providing us with the rainfall data used in this research.

Authors contributions

All authors have contributed equally to prepare the paper.

Availability of data and materials

The data that support the findings of this study are available from the corresponding author upon reasonable request.

Conflict of interests

The authors declare that they have no known competing financial interests or personal relationships that could have appeared to influence the work reported in this paper.

References

Abaoui J., Ghmari A. E., El Harti A. E., Bachaoui E. M., Bannari A., El Bouadili A. (2005) Mapping of water erosion in mountainous areas: case of the AïtBouGoumez watershed, High Atlas, Morocco. *Estudios Geológicos* 61:33–39. https://doi.org/10.3989/egeol.05611-240

Ait Haddou M., Bouchriti Y., Ikirri M., et al. (2023) Delineation of groundwater potential zones in a semi-arid region using remote sensing and GIS: A case study of Argana Corridor (Morocco), in advanced technology for smart environment and energy. *Environmental Science and Engineering, Springer, Cham.,* pp. 257–268. https://doi.org/10.1007/978-3-031-25662-2-21

Ait Haddou M., El Caid M. B., Aydda A., Bouchriti Y., Wanaim A., Gougueni H., Ezaidi S. (2022a) Fencing land impacts on plant biodiversity and argan trees dynamic in the Ida-Ou-Tanane (central western of Morocco). *IOP Conference Series: Earth and Environmental Science* 1090:012023. https://doi.org/10.1088/17551315/1090/1/012023

Ait Haddou M., Kabbachi B., Aydda A., BouchritiY H. Gougueni, En-Naciry M., Aichi A. (2022b) Traditional practices: A window for water erosion management in the Argana basin (Western High Atlas Morocco). *E3S Web of Conferences* 337:02002. https://doi.org/10.1051/e3sconf/202233702002

Ait Haddou M., Kabbachi B., Aydda A., Gougni H., Bouchriti Y. (2020) Spatial and temporal rainfall variability and erosivity: Case of the Issen watershed, SW-Morocco. *E3S Web of Conferences* 183:02003. https://doi.org/10.1051/e3sconf/202018302003

Ait Haddou M., Wanaim A., Ikirri M., Aydda A., Bouchriti Y., Abioui M., Kabbachi B. (2022c) Digital elevation model-derived morphometric indices for physical characterization of the Issen Basin (Western High Atlas of Morocco). *Ecological Engineering & Environmental Technology* 23 (5): 285–298. https://doi.org/10.12912/27197050/152161

Alahiane N., Elmouden A., Aitlhaj A., Boutaleb S. (2016) Small dam reservoir siltation in the Atlas Mountains of Central Morocco: analysis of factors impacting sediment yield. *Environmental Earth Sciences* 75:1035. https://doi.org/https://doi.org/10.1007/s12665-016-5795-y

Amini H., Honarjoo N., Jalaliyan A., Khalilizadeh M., Baharlouie J. (2014) A comparison of EPM and WEPP models for estimating soil erosion of Marmeh Watershed in the South Iran. *Agriculture and Forestry* 60 (4): 299–315.

Amini S., Rafiei B., Khodabakhsh S., Heydari M. (2010) Estimation of erosion and sediment yield of Ekbatan Dam drainage basin with EPM, using GIS. *Iranian Journal of Earth Sciences* 2 (2): 173–180.

Aouichaty N., Bouslihim Y., Hilali S., Zouhri A., Koulali Y. (2022) Estimation of water erosion in abandoned quarries sites using the combination of RUSLE model and geostatistical method. *Scientific African* 16:e01153. https://doi.org/10.1016/j.sciaf.2022.e01153

Aswathi J., Sajinkumar K. S., Rajaneesh A., al. et (2022) Furthering the precision of RUSLE soil erosion with PSInSAR data: an innovative model. *Geocarto International* 37 (27): 16108–16131. https://doi.org/10.1080/10106049.2022.2105407

Ayt Ougougdal H., Khebiza M. Y., Messouli M., Bounoua L. (2020) Delineation of vulnerable areas to water erosion in a mountain region using SDR-InVEST model: A case study of the Ourika watershed, Morocco. *Scientific African* 10:e00646. https://doi.org/10.1016/j.sciaf.2020.e00646

Benavidez R., Jackson B., Maxwell D., Norton K. (2018) A review of the (Revised) Universal Soil Loss Equation ((R)USLE): with a view to increasing its global applicability and improving soil loss estimates. *Hydrology and Earth System Sciences* 22 (11): 6059–6086. https://doi.org/10.5194/hess-22-6059-2018

Bensekhria A., Bouhata R. (2022) Assessment and mapping soil water Erosion using RUSLE approach and GIS tools: Case of Oued el-Hai Watershed, Aurès West, Northeastern of Algeria. *ISPRS International Journal of Geo-Information* 11 (2): 84. https://doi.org/10.3390/ijgi11020084

Bosco C., Rigo D. de, Dewitte O., Poesen J., Panagos P. (2015) Modelling soil erosion at European scale: towards harmonization and reproducibility. *Natural Hazards and Earth System Sciences* 15 (2): 225–245. https://doi.org/10.5194/nhess-15-225-2015

Bou-imajjane L., Belfoul M. A. (2020) Soil loss assessment in Western High Atlas of Morocco: Beni Mohand Watershed study case. *Applied and Environmental Soil Science,* 1–15. https://doi.org/10.1155/2020/6384176

Brahim B., Meshram S. G., Abdallah D., et al. (2020) Mapping of soil sensitivity to water erosion by RUSLE model: case of the Inaouene watershed (Northeast Morocco). *Arabian Journal of Geosciences* 13:1153. https://doi.org/10.1007/s12517-020-06079-y

Cavallar W. (1950) Preliminary sketch of the Soil Map of Morocco - ESDAC - European Commission.

Ebadati N., Shafiei Motlagh K., Khoshmanesh B., Razavian F. (2022) Estimation of erosion and sedimentation using EPM and geomorphology models in a semi-arid environment (case study: Qir, Karzin basin of Iran). 81:396. 15 https://doi.org/10.1007/s12665-022-10521-7

El Jazouli A., Barakat A., Khellouk R., Rais J., El Baghdadi M. (2019) Remote sensing and GIS techniques for prediction of land use land cover change effects on soil erosion in the high basin of the Oum Er Rbia River (Morocco). *Remote Sensing Applications: Society and Environment* 13:361–374. https://doi.org/10.1016/j.rsase.2018.12.004

Elaloui A., Marrakchi C., Fekri A., Maimouni S., Aradi M. (2017) USLE-based assessment of soil erosion by water in the watershed upstream Tessaoute (Central High Atlas, Morocco). *Modeling Earth Systems and Environment* 3:873–885. https://doi.org/10.1007/s40808-017-0340-x

Fernandez C., Wu J. Q., McCool D. K., Stöckle C. O. (2003) Estimating water erosion and sediment yield with GIS, RUSLE, and SEDD. *Journal of soil and Water Conservation* 58:128–136.

Fistikoglu O., Harmancioglu N. B. (2002) Integration of GIS with USLE in assessment of soil Erosion. *Water Resources Management* 16:447–467. https://doi.org/10.1023/A:1022282125760

Ganasri B. P., Ramesh H. (2016) Assessment of soil erosion by RUSLE model using remote sensing and GIS - A case study of Nethravathi Basin. *Geoscience Frontiers* 7:953–961. https://doi.org/10.1016/j.gsf.2015.10.007

Gaubi I., Chaabani A., Ben Mammou A., Hamza M. H. (2017) A GIS-based soil erosion prediction using the Revised Universal Soil Loss Equation (RUSLE) (Lebna watershed, Cap Bon, Tunisia). *Natural Hazards* 86:219–239. https://doi.org/10.1007/s11069-016-2684-3

Gavrilović S. (1972) Engineering of torrents and erosion.

Getachew B., Manjunatha B. R., Bhat G. H. (2021) Assessing current and projected soil loss under changing land use and climate using RUSLE with Remote sensing and GIS in the Lake Tana Basin, Upper Blue Nile River Basin, Ethiopia. *Egyptian Journal of Remote Sensing and Space Science* 24:907–918. https://doi.org/10.1016/j.ejrs.2021.10.001

Getu L. A., Nagy A., Addis H. K. (2022) Soil loss estimation and severity mapping using the RUSLE model and GIS in Megech watershed, Ethiopia. *Environmental Challenges* 8:100560. https://doi.org/10.1016/j.envc.2022.100560

Ghosal K., Das Bhattacharya S. (2020) A review of RUSLE model. *Journal of the Indian Society of Remote Sensing* 48:689–707. https://doi.org/10.1007/s12524-019-01097-0

Hao H., Wang J., Guo Z., Hua L. (2019) Water erosion processes and dynamic changes of sediment size distribution under the combined effects of rainfall and overland flow. *CATENA* 173:494–504. https://doi.org/10.1016/j.catena.2018.10.029

Haregeweyn N., Poesen J., Verstraeten G., et al. (2013) Assessing the performance of a spatially distributed soil erosion and sediment delivery model (Watem/Sedem) in northern Ethiopia: spatially distributed soil erosion and sedimentation. *Land Degradation & Development* 24:188–204. https://doi.org/10.1002/ldr.1121

HCEFLCD (2011) High Commission for Water and Forests and the Fight against Desertification (HCEFLCD). *National Watershed Management Plan: Summary and Conclusions of the Synthesis Report*

Javanbakht M., Asadi V., Dabiri R. (2020) Evaluation of hydrogeochemical characteristics and evolutionary process of groundwater in Jajarm Plain, northeastern Iran. *Environment and Water Engineering* 6 (3): 206–218. https://doi.org/10.22034/jewe.2020.232598.1366

Jehangir Khan M., Ghazi S., Mehmood M., Yazdi A., Naseem A. A., Serwar U., Zaheer A., Ullah H. (2021) Sedimentological and provenance analysis of the Cretaceous Moro formation Rakhi Gorge, Eastern Sulaiman Range, Pakistan. *Iranian Journal of Earth Sciences* 13 (4): 252–266. https://doi.org/10.30495/ijes.2021.1917721.1564

Joghatayi H., Dabiri R., Moslempour M. E., Otari M., Sharifiyan Attar R. (2015) Groundwater quality assessment using the Groundwater Quality Index and GIS in Joghatay plain, NE Iran. *Human & Environment* 13 (4): 17–25.

Kang S., Zhang L., Song X., Zhang S., Liu X., Liang Y., Zheng S. (2001) Runoff and sediment loss responses to rainfall and land use in two agricultural catchments on the Loess Plateau of China. *Hydrological Processes* 15:977–988. https://doi.org/10.1002/hyp.191

Khemiri K., Jebari S. (2021) Water erosion assessment in watersheds of the Tunisian semi-arid area with RUSLE and MUSLE models coupled with a Geographic Information System. *Cahiers Agricultures* 30:1–11. https://doi.org/10.1051/cagri/2020048

Kifelew M. S., Mesalie R. A., Shumey E. E., Mekash S., Fikadie F. T., Worku T. A., et al. (2022) Identification of erosion hot spot area using GIS and gully contribution for reservoir sedimentation in the case of Abrajit reservoir, Upper Blue Nile Basin, Ethiopia. *Sustainable Water Resources Management* 8:93. https://doi.org/10.1007/s40899-022-00680-7

Knijff J. M. Van der, Jones R. J. A., Montanarella L. (2000) Soil Erosion Risk Assessment in Europe- ESDAC-European Commission.

Labbaci A., Moukrim S., Lahssini S., Laaribiya S., Alaoui H. M. (2020) An assessment of soil erosion in Westem High Atlas of Morocco: an application to Ain Asmama site. *IEEE International conference of Moroccan Geomatics (Morgeo), IEEE, Casablanca* 2020:1–6. https://doi.org/10.1109/Morgeo49228.2020.9121906

Lamane H., Moussadek R., Baghdad B., Mouhir L., Briak H., Laghlimi M., Zouahri A. (2022) Soil water erosion assessment in Morocco through modeling and fingerprinting applications: A review. *Heliyon* 8 (8): e10209. https://doi.org/10.1016/j.heliyon.2022.e10209

Leh M., Bajwa S., Chaubey I. (2013) Impact of land use change on erosion risk: an integrated remote sensing, geographic information system and modeling methodology: impact of land use change on erosion risk. *Land Degradation & Development* 24:409–421. https://doi.org/10.1002/ldr.1137

Ligonja P. J., Shrestha R. P. (2015) Soil Erosion assessment in Kondoa Eroded Area in Tanzania using Universal Soil Loss Equation, Geographic information systems and socioeconomic approach. *Land Degradation & Development* 26:367–379. https://doi.org/10.1002/ldr.2215

Lu D., Li G., Valladares G. S., Batistella M. (2004) Mapping soil erosion risk in Rondônia, Brazilian Amazonia: using RUSLE, remote sensing and GIS. *Land Degradation & Development* 15:499–512. https://doi.org/10.1002/ldr.634

Meliho M., Khattabi A., Mhammdi N. (2020) Spatial assessment of soil erosion risk by integrating remote sensing and GIS techniques: a case of Tensift watershed in Morocco. *Environmental Earth Sciences* 79:1–19. https://doi.org/10.1007/s12665-020-08955-y

Merritt W. S., Letcher R. A., Jakeman A. J. (2003) A review of erosion and sediment transport models. *Environmental Modelling & Software* 18:761–799. https://doi.org/10.1016/S1364-8152(03)00078-1

Mhangara P., Kakembo V., Lim K. J. (2012) Soil erosion risk assessment of the Keiskamma catchment, South Africa using GIS and remote sensing. *Environmental Earth Sciences* 65:2087–2102. https://doi.org/https://doi.org/10.1007/s12665-011-1190-x

Mitasova H., Hofierka J., Zlocha M., Iverson L. R. (1996) Modelling topographic potential for erosion and deposition using GIS. *International Journal of Geographical Information Systems* 10:629–641. https://doi.org/10.1080/02693799608902101

Mlih Ben, Laadila M., Kochri A. E., El Youssi M., El Kochri A., Nassili M. (2004) Permian and Triassic synrift filling of the Tahanaout basin (High Atlas of Marrakech Morocco)geodynamics and sedimentary organization. *Estudios Geológicos* 60:123–138. https://doi.org/10.3989/egeol.04603-685

Mukanov Y., Chen Y., Baisholanov S., et al. (2019) Estimation of annual average soil loss using the Revised Universal Soil Loss Equation (RUSLE) integrated in a Geographical Information System (GIS) of the Esil River basin (ERB), Kazakhstan. *Acta Geophysica* 67:921–938. https://doi.org/10.1007/s11600-019-00288-0

Ochoa P. A., Fries A., Mejía D., et al. (2016) Effects of climate, land cover and topography on soil erosion risk in a semiarid basin of the Andes. *CATENA* 140:31–42. https://doi.org/10.1016/j.catena.2016.01.011

Olsen P. E., Kent D. V., Et-Touhami M., Puffer J. (2003) Cyclo-, magneto-, and bio-stratigraphic constraints on the duration of the CAMP event and its relationship to the Triassic-Jurassic boundary. In: Hames W, McHone JG, Renne P, Ruppel C (eds) Geophysical Monograph Series. *American Geophysical Union, Washington, DC* 7:32.

Panagos P., Borrelli P., Meusburger K., Alewell C., Lugato E., Montanarella L. (2015) Estimating the soil erosion cover-management factor at the European scale. *Land Use Policy* 48:38–50. https://doi.org/10.1016/j.landusepol.2015.05.021

Panagos P., Borrelli P., Meusburger K., Yu B., Klik A., et al. (2017) Global rainfall erosivity assessment based on high-temporal resolution rainfall records. *Scientific Reports* 7:1–12. https://doi.org/10.1038/s41598-017-04282-8

Phinzi K., Ngetar N. S. (2019) The assessment of water-borne erosion at catchment level using GIS-based RUSLE and remote sensing: A review. *International Soil and Water Conservation Research* 7:27–46. https://doi.org/10.1016/j.iswcr.2018.12.002

Renard K. G. (1997) Predicting soil erosion by water: a guide to conservation planning with the revised universal soil loss equation (RUSLE). *USA (eds)*

Renard K. G., Freimund J. R. (1994) Using monthly precipitation data to estimate the R-factor in the revised USLE. *Journal of Hydrology* 157:287–306.

Rey F., Ballais J. L., Marre A., Rovéra G. (2004) The role of vegetation in protection against surface hydric erosion. *Comptes Rendus Géoscience* 336:991–998. https://doi.org/10.1016/j.crte.2004.03.012

Rezapour Tabari M. M., Yazdi A. (2014) Conjunctive use of surface and groundwater with inter-basin transfer approach: case study Piranshahr. *Water Resources Management* 28:1887–1906. https://doi.org/10.1007/s11269-014-0578-2

Sadiki A., Bouhlassa S., Auajjar J., Faleh A., Macaire J. J. (2004) Evaluation and cartography of erosion risks by the Universal soil loss equation using a GIS in Eastern Rif (Morocco): case of oued Boussouab Watershed. *Bulletin de l'Institut Scientifique, Rabat, section Sciences de la Terre* 26:69–79.

Saha M., Sauda S. S., Real H. R. K., Mahmud M. (2022) Estimation of annual rate and spatial distribution of soil erosion in the Jamuna basin using RUSLE model: A geospatial approach. *Environmental Challenges* 8:1–14. https://doi.org/10.1016/j.envc.2022.100524

Salhi A., Benabdelouahab T., Martin-Vide J., Okacha A., El Hasnaoui Y., El Moussaoui M., El Morabit A., et al. (2020) Bridging the gap of perception is the only way to align soil protection actions. *Science of The Total Environment* 718:137421. https://doi.org/10.1016/j.scitotenv.2020.137421

Stanchi S., Falsone G., Bonifacio E. (2015) Soil aggregation, erodibility, and erosion rates in mountain soils (NW Alps, Italy). *Solid Earth* 6:403–414. https://doi.org/10.5194/se-6-403-2015

Tahiri M., Tabyaoui H., Hammichi F. E., Achab M., Tahiri A., El Hadi H. (2017) Quantification of water erosion and sedimentation using empirical models in the Tahaddart watershed Northwestern Rif, Morocco. *Bulletin de l'Institut Scientifique, Rabat, Section Sciences de la Terre* 39:87–101.

Tairi A., Elmouden A., Bouchaou L., Aboulouafa M. (2021) Mapping soil erosion–prone sites through GIS and remote sensing for the Tifnout Askaoun watershed, southern Morocco. *Arabian Journal of Geosciences* 14:811. https://doi.org/10.1007/s12517-021-07009-2

Talchabhadel R., Prajapati R., Aryal A., et al. (2020) Assessment of rainfall erosivity (R-factor) during 1986-2015 across Nepal: a step towards soil loss estimation. *Environ Monit Assess* 192:1–17. https://doi.org/10.1007/s10661-020-8239-9

Tixeront M., Duffaud F. (1977) Geological map and mineralization of the Argana corridor, Western High Atlas. *Service géologique du Maroc*

Tribak A., El Garouani A., Abahrour M. (2009) Quantitative evaluation of water erosion in the marly soils of the eastern Pre-Rif (Morocco): case of the Oued Tlata sub-basin. *Sécheresse* 20:333–337.

Ustaoğlu B., İkiel C., Atalay Dutucu A., Koç D. E. (2021) Erosion susceptibility analysis in Datça and Bozburun Peninsulas, Turkey. *Iranian Journal of Science and Technology, Transactions A: Science* 45:557–570. https://doi.org/10.1007/s40995-020-01053-5

Wischmeier W. H., Smith D. D. (1978) Predicting Rainfall Erosion Losses: A guide to conservation planning. USDA agricultural handbook. *U.S. Gov. Print. Office, Washington, DC.* 537

Zhao X., Dupont L., Cheddadi R., Kölling M., Reddad H., Groeneveld J., Ain-Lhout F. Z., Bouimetarhan I. (2019) Recent climatic and anthropogenic impacts on endemic species in southwestern Morocco. *Quaternary Science Reviews* 221:105889. https://doi.org/10.1016/j.quascirev.2019.105889